Applied Physics Letters

NO_2 gas sensor based on hydrogenated graphene

Cite as: Appl. Phys. Lett. **111**, 213102 (2017); https://doi.org/10.1063/1.4999263
Submitted: 07 August 2017 . Accepted: 05 November 2017 . Published Online: 20 November 2017

Sungjin Park, Minji Park, Sunghyun Kim, Sum-Gyun Yi, Myeongjin Kim, Jangyup Son, Jongin Cha, Jongill Hong, and Kyung-Hwa Yoo

AIP Publishing

NO_2 gas sensor based on hydrogenated graphene

Sungjin Park,[1] Minji Park,[1] Sunghyun Kim,[1] Sum-Gyun Yi,[1] Myeongjin Kim,[1] Jangyup Son,[2] Jongin Cha,[2] Jongill Hong,[2,a)] and Kyung-Hwa Yoo[1,a)]
[1]*Department of Physics, Yonsei University, Seoul 03722, South Korea*
[2]*Department of Materials Science and Engineering, Yonsei University, Seoul 03722, South Korea*

(Received 7 August 2017; accepted 5 November 2017; published online 20 November 2017)

We investigated the relationship between defects in graphene and NO_2 gas sensitivity of graphene-based gas sensors. Defects were introduced by hydrogen plasma or ultraviolet (UV)/ozone treatment. As the defect concentration increased, the sensitivity was enhanced, and sub-ppb level detection limit was achieved. UV irradiation was used for recovery at room temperature. However, defects generated by ozone treatment, like graphene oxide, were reduced back to graphene by UV irradiation, so the ozone-treated graphene sensor was not stable over time. In contrast, the response of the hydrogenated graphene sensor was very repeatable because defects generated by hydrogenation was stable enough not to be dehydrogenated by UV irradiation. These results demonstrate that the hydrogenated graphene sensor is a highly sensitive and stable NO_2 sensor at room temperature. *Published by AIP Publishing.* https://doi.org/10.1063/1.4999263

Graphene has recently received considerable attention because of their novel electrical, mechanical, and chemical properties.[1–3] In particular, electron transport through graphene is highly sensitive to the presence of adsorbed molecules owing to the two-dimensional structure of graphene, so graphene has been extensively studied as a sensing material to detect various gases, such as NH_3, NO_2, CO, SO_2, and H_2S.[4–9] The operational principle of graphene-based sensors is to measure a change in the electrical conductance due to gas molecules adsorbed on graphene's surface and acting as donors or acceptors.[5] To improve the sensing performance of graphene sensors, various methods were reported. For example, graphene surface was modified by metal nanoparticles[6] and organic polymers,[7] and patterned into nanostructure mesh.[8] In addition, the graphene was treated with ultraviolet (UV)/ozone to introduce oxygen defects.[9]

Here, we report a hydrogenated graphene sensor (HGS) that can detect nitrogen dioxide (NO_2) gas, one of the main air pollutants, in sub-ppb levels. The HGS was prepared by treating the pristine graphene sensor (PGS) with hydrogen plasma, and the defects generated by hydrogenation were characterized by Raman spectroscopy. For comparison, we also fabricated the ozone-treated graphene sensor (OGS). For both sensors, the sensitivity increased with the increase in defect concentration in graphene, as expected from theoretical studies that the defect sites cause localized perturbations in the structure and electronic states of graphene, and lead to higher binding energy and charge transfer between graphene and gas molecules.[10,11] However, the response of the OGS was not repeatable since the UV irradiation adopted for recovery caused reduction of graphene oxide. On the other hand, the HGS was very stable under repeated UV irradiation since the hydrogenated graphene could not be dehydrogenated to graphene by UV irradiation. Moreover, its sensitivity was higher than that of the OGS, demonstrating that the HGS could provide better sensing performance than the OGS. In addition, we investigated the relationship between the defect concentration in graphene and the sensitivity of various graphene-based sensors.

We fabricated the PGS on a Si substrate with a 300-nm-thick thermally grown SiO_2 layer [inset of Fig. 1(a)]. Graphene was grown on a 50-μm-thick copper (Cu) foil using a chemical vapor deposition (CVD) method.[12] Briefly, the Cu foil was annealed at 850 °C at low pressure with a H_2 flow of 40 sccm for 30 min to remove CuO from the Cu foil surface, and then graphene was grown at 850 °C by introducing C_2H_2:H_2 (5:35 sccm) gas for 30 min. After the growth, the graphene was cooled to room temperature under an Ar flow of 200 sccm. This CVD-grown graphene was transferred onto a Si/SiO_2 substrate by a poly(methyl methacrylate) transfer method.[13] Then, a $1.5 \times 1.5\ \mu m^2$ graphene channel was patterned using electron-beam lithography and etched with O_2 plasma (100 sccm, 30 W, and 30 s). Au/Cr (50 nm/5 nm) electrodes were made by electron-beam lithography and lift-off techniques. The HGS was prepared by treating the PGS with hydrogen plasma.[14] The hydrogen plasma was generated in a separate gun with a microwave power of 180 W at 2.5 GHz and a H_2 flow of 25 sccm, and the PGS was positioned 10 cm downstream of the end of the gun.

For gas sensing experiments, we constructed a small chamber with electrical feedthrough and optical window. To measure the sensing performance, various concentrations of NO_2 gas were injected into the chamber by adjusting the ratio of the flow rate of NO_2 gas to air using mass flow controllers (MFCs). To recover the sensor, air alone was supplied into the chamber. All measurements were performed at room temperature (25 ± 2 °C), and electrical measurements were carried out using a semiconductor parameter analyzer (Keithley 4200).

Figure 1(a) shows a current-voltage (I-V) curve of the PGS. The I-V curve was linear, and the current-gate voltage (I-V_G) transfer curve exhibited an ambipolar behavior with a Dirac point near $V_G \approx 0$ V [Fig. 1(b)], where the Si substrate was used as the gate electrode. The Raman spectrum measured before patterning showed two characteristic graphene peaks, G and 2D, at ~1580 and ~2680 cm^{-1}, respectively

a)Authors to whom correspondence should be addressed: Hong.jongill@yonsei.ac.kr and khyoo@yonsei.ac.kr

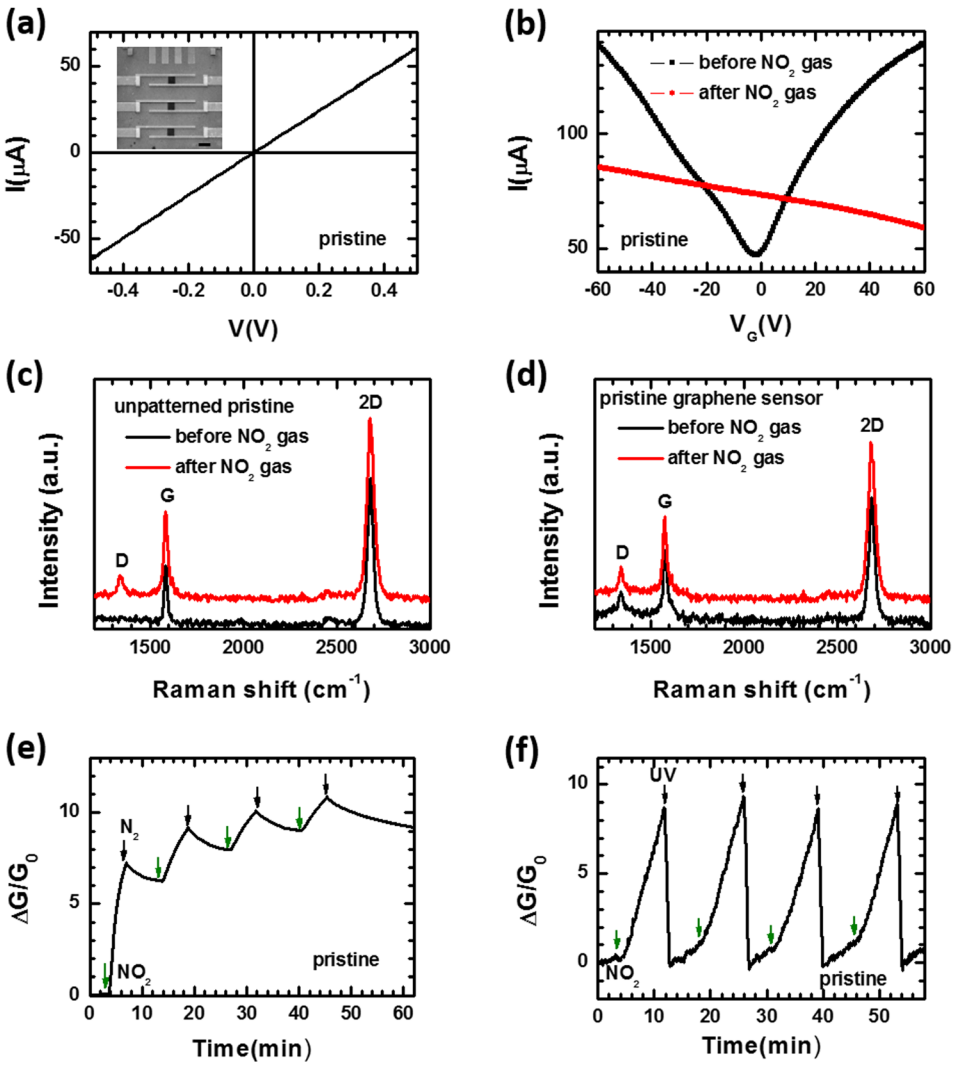

FIG. 1. (a) *I-V* curve of the PGS. Inset shows a field emission scanning electron microscope image of the fabricated PGS. The scale bar is 2 μm. (b) *I-V*$_G$ transfer curves of the PGS before and after exposure to NO_2 gas. Raman spectra of (c) unpatterned pristine graphene and (d) PGS before and after exposure to NO_2 gas. The spectra are offset vertically for clarity. (e) Real-time response of the PGS when alternately exposed to 1 ppm NO_2 gas diluted in air and to air alone. Green arrows indicate the times that 1 ppm NO_2 was added and black arrows show the times that NO_2 gas was shut off. (f) Real-time response of the PGS when alternately exposed to 1 ppm NO_2 gas diluted in air and irradiated by UV light. Green arrows indicate the times that 1 ppm NO_2 was added and black arrows show the times that NO_2 gas was shut off and UV light was irradiated.

[Fig. 1(c)]. The intensity ratio of the 2D peak to the G peak (I_{2D}/I_G) was about 3.2, indicating single-layer graphene.[15] On the other hand, the patterned graphene sensor exhibited an additional D peak at $\sim$1350 cm^{-1}, which was ascribed to graphene edges or defects generated during the patterning process [Fig. 1(d)].

Figure 1(e) shows the real-time response ($\Delta G(t)/G_0$) of the PGS when the sensor was alternately exposed to 1 ppm NO_2 gas and to dry air, where G_0 is the conductance at $t = 0$, and $\Delta G(t) = G(t) - G_0$. Upon exposure to NO_2 gas, the conductance increased by about 8%, as reported by others.[8,9] However, when the NO_2 gas was shut off, the conductance was not restored to the initial value. According to a theoretical computation,[11] a physisorption energy was estimated to be approximately -0.48 eV for NO_2 on the graphene sheet. Thus, most NO_2 molecules might not be desorbed at room temperature, resulting in incomplete recovery. To improve the recovery characteristics, the sensor was irradiated by UV light ($\lambda = 254$ nm, 20 mW/cm^2) since UV light has an energy of 4.9 eV. Indeed, the conductance recovered to nearly the initial value upon UV irradiation, indicating that NO_2 molecules were desorbed from the graphene surface by UV irradiation [Fig. 1(f)]. Compared to the gas sensors based on layered transition metal dichalcogenides, such as MoS_2[16,17] and WS_2,[18] the PGS exhibited a higher sensitivity and a faster response.

Next, we prepared the OGS by treating the PGS with UV/ozone generated by an ozone generator (254 nm with an intensity of 30 mW/cm^2). Raman spectra obtained from the OGS revealed four characteristics: an increase in I_D/I_G, a decrease in I_{2D}/I_G, and the onset of an additional D′ peak at $\sim$1620 cm^{-1} and a combination mode (D + D′) at $\sim$2950 cm^{-1} [Fig. 2(a)]. These results indicate that defects, such as sp^3 C-O bonds and/or broken symmetry in the carbon sp^2 network, were introduced by ozonation, as the D and D′ peaks require defects for their activation via intervalley and intravalley double-resonance Raman processes, respectively.[19,20] As the exposure time increased, the intensity ratio I_D/I_G increased and the electrical conductance decreased [Fig. 2(b)]. Because I_D/I_G provides a convenient measure of the amount of defects in graphene,[19] these results indicate that more defects were generated as the treatment time increased. However, when the treatment time was longer than 120 s, an insulating behavior appeared. Thus, the final OGS was prepared using UV/ozone treatment for 90 s.

Figure 2(c) shows the real-time response measured repeatedly at 1 day intervals for the OGS when the OGS was alternately exposed to different concentrations of NO_2 gas and irradiated by UV light, where G_0 is the initial conductance on the first day. As the NO_2 concentration increased, $\Delta G/G_0$ increased and UV irradiation induced nearly complete

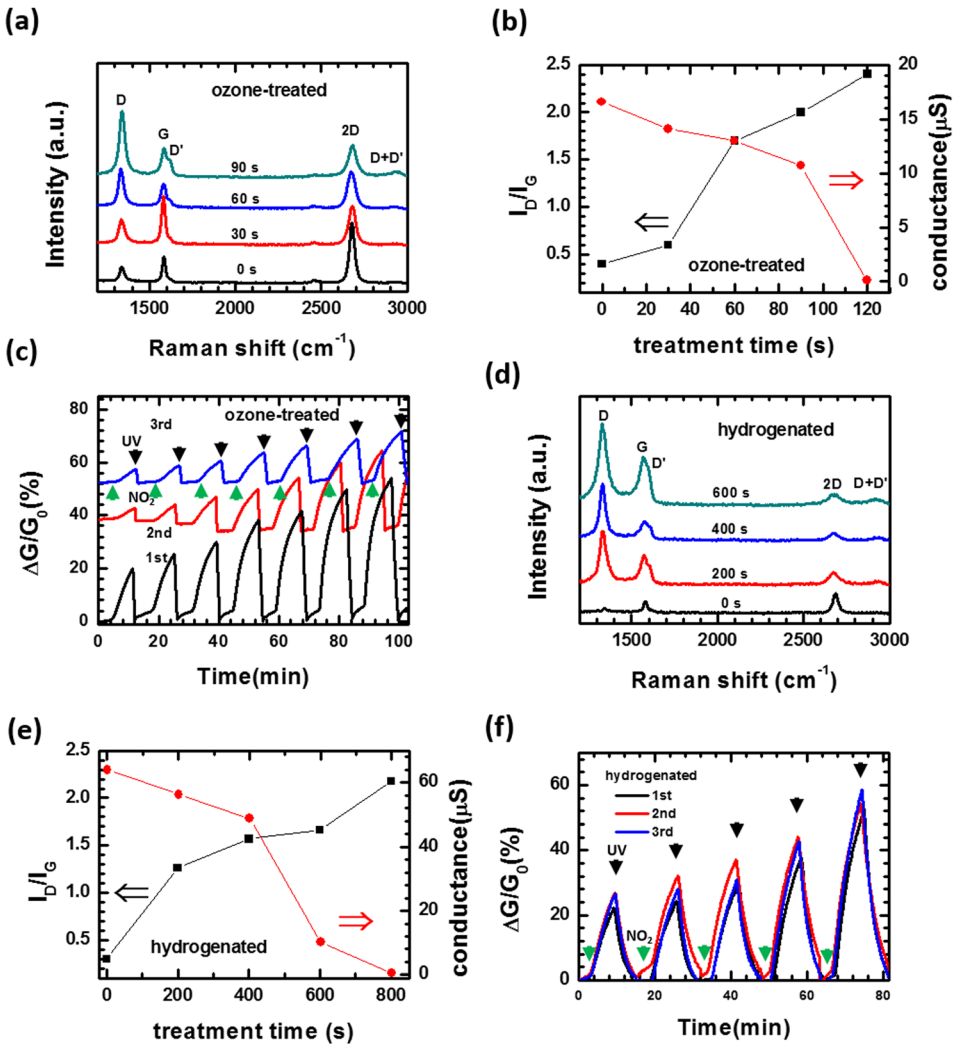

FIG. 2. (a) Raman spectra obtained from the OGS after treatment with UV/ozone for different times. The spectra are offset vertically for clarity. (b) Intensity ratio I_D/I_G and the conductance as a function of treatment time for the OGS. (c) Real-time response of the OGS measured repeatedly at 1 day intervals at different concentrations of NO_2 gas diluted in air. Green arrows indicate the times that NO_2 at concentrations of 0.4, 0.6, 1, 2, 4, 8, and 12 ppm was added, and black arrows show the times of UV irradiation. (d) Raman spectra obtained from the HGS after treatment with hydrogen plasma for different times. The spectra are offset vertically for clarity. (e) Intensity ratio I_D/I_G and the conductance as a function of treatment time for the HGS. (f) Real-time response of the HGS measured repeatedly at 1 day intervals at different concentrations of NO_2 gas diluted in air gas. Green arrows indicate the times that NO_2 at concentrations of 0.4, 0.6, 1, 2, and 4 ppm was added, and black arrows show the times that NO_2 gas was shut off and UV light was irradiated.

recovery, as for the PGS. In addition, the first-day measurements showed that the OGS was more sensitive than the PGS, probably because of defects introduced by UV/ozone treatment (Fig. S1), as reported by others.[9] However, when similar real-time response measurements were repeated the next day, the conductance of the OGS increased and $\Delta G/G_0$ decreased, while the PGS showed nearly reproducible values of $\Delta G/G_0$ (see supplementary material, Fig. S1). To understand this instability, we measured the Raman spectra of the OGS after each real-time response measurement (Fig. S2). Initially, I_D/I_G was larger than 1; however, it became less than 1 starting on day 3. These results imply that graphene oxide was reduced through UV irradiation, resulting in an increase in the conductance and a decrease in the sensitivity.

To circumvent this instability problem, we fabricated the HGS by treating the PGS with hydrogen plasma. Raman spectra obtained from the HGS showed characteristics similar to those of the OGS. These results suggested that similar types of defects were introduced by hydrogenation and ozonation [Fig. 2(d)], although UV/ozone treatment or hydrogenation did not induce a noticeable change in the microstructure of graphene (Fig. S3). The final HGS was prepared by exposing the PGS to hydrogen plasma for 600 s because an HGS treated for longer than 800 s had nearly zero conductance [Fig. 2(e)]. From $I_D/I_G \approx 2.2$ measured for the HGS, the hydrogen coverage was estimated to be approximately 15%.[14] To test the stability, real-time response measurements were repeated at 1 day intervals, as for the OGS [Fig. 2(f)]. In contrast to the OGS, the HGS yielded reproducible values of $\Delta G/G_0$, demonstrating that the HGS was stable at room temperature under repeated UV irradiation. The binding energies of C-H and C-O bonds are ~6.56 eV and ~3.71 eV, respectively,[21,22] so the hydrogenated graphene could not be dehydrogenated to graphene by UV irradiation.

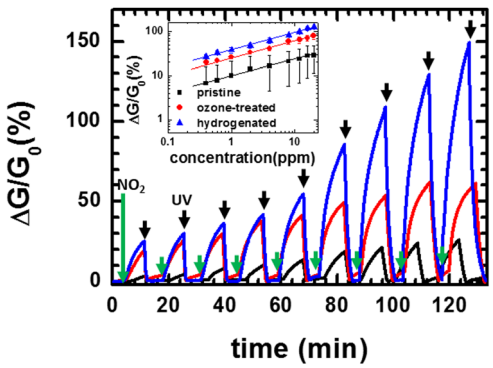

FIG. 3. Real-time response of the PGS, HGS, and OGS measured at different NO_2 concentrations. Green arrows indicate the times that NO_2 at concentrations of 0.4, 0.6, 1, 2, 4, 8, 12, and 20 ppm was added, and black arrows show the times NO_2 gas was shut off and UV light was irradiated. The inset shows a plot of $\Delta G/G_0$ versus NO_2 concentration on a logarithmic scale for the PGS, HGS, and OGS.

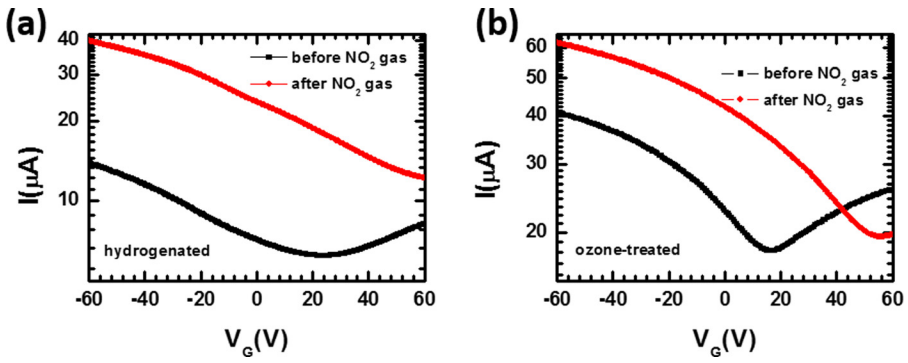

FIG. 4. I-V_G transfer curves of (a) HGS and (b) OGS measured before and after exposure to NO_2 gas.

In Fig. 3, representative real-time responses of the PGS, OGS, and HGS measured at different concentrations of NO_2 gas are compared, where the OGS data were obtained from the first measurement. The HGS was more sensitive than the OGS, and the OGS was more sensitive than the PGS. The inset in Fig. 3 plots $\Delta G/G_0$ versus the NO_2 concentration on a logarithmic scale. The relationship between $\Delta G/G_0$ and the NO_2 concentration was described by the Freundlich adsorption equation, $\Delta G/G_0 \propto c^n$, where c is the gas concentration and n is an exponent.[23] The value of n was estimated to be approximately 0.4 for all the sensors. For a 1 ppb NO_2 concentration, $\Delta G/G_0$ was estimated to be approximately 0.9, 2.5, and 4% for the PGS, OGS, and HGS, respectively. These results deduce that a sub-ppb concentration is clearly and reproducibly detectable using the HGS (Fig. S4).

I-V_G transfer curves measured before and after exposure to NO_2 gas are shown in Figs. 4(a) and 4(b) for the HGS and OGS, respectively. Compared to the PGS, the HGS and OGS showed Dirac points at more positive V_G values even before exposure to NO_2 gas; this behavior was ascribed to the p-type doping caused by hydrogenation or ozonation.[14,22] Upon exposure to NO_2 gas, the Dirac point shifted further to more positive V_G values for both sensors. Furthermore, the HGS exhibited a larger shift in the Dirac point than the OGS, suggesting that more charges were transferred to adsorbed NO_2 molecules from the HGS than from the OGS. As a result, higher sensitivity could be achieved for the HGS than for the OGS.

Raman spectra were also measured before and after exposure to NO_2 gas without UV irradiation. For unpatterned pristine graphene, the D peak appeared at $\sim$1350 cm^{-1} after exposure to NO_2 gas, indicating that defects or disorders were introduced by adsorption of NO_2 molecules on the graphene surface [Fig. 1(c)]. On the other hand, for all the patterned sensors, the I_D/I_G values were nearly unchanged by exposure to NO_2 gas [Fig. 1(d)]. NO_2 molecules might be preferentially adsorbed on existing defect sites that form low-energy adsorption sites,[10,11] so I_D/I_G was not changed by exposure to NO_2 gas.

In addition, we plotted $\Delta G/G_0$ as a function of I_D/I_G for various graphene-based sensors to investigate the relationship between the sensitivity and the defect concentration in graphene, where $\Delta G/G_0$ was measured under 1 ppm NO_2 gas (Fig. 5). $\Delta G/G_0$ increased with increasing I_D/I_G, supporting the suggestion that the gas reactivity was improved by the presence of defects in graphene. However, different levels of sensitivity were observed depending on the value of I_{2D}/I_G that was estimated before hydrogenation or ozonation. The sensors with $I_{2D}/I_G > 2$ exhibited higher sensitivity at similar values of I_D/I_G than the sensors with $I_{2D}/I_G < 2$, indicating that the sensitivity also depended on the quality of the graphene.

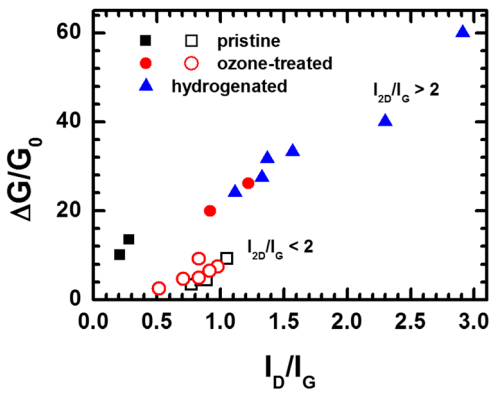

FIG. 5. $\Delta G/G_0$ versus I_D/I_G for various graphene-based sensors. The solid symbols denote $I_{2D}/I_G > 2$ and the open ones indicate $I_{2D}/I_G < 2$.

In summary, we fabricated the HGS and OGS by treating the PGS with indirect hydrogen plasma and UV/ozone, respectively, to improve the sensing performance of the PGS. Raman spectroscopy analysis revealed that sp^3 types of defects were introduced by ozonation and hydrogenation. The introduced defects contributed to the sensitivity enhancement, so the sensitivity increased with increasing number of defects. However, the OGS was not stable owing to reduction of graphene oxide by the UV irradiation adopted for recovery. In contrast, the HGS exhibited reproducible sensing performance at room temperature. Furthermore, the detection limit of the HGS was estimated to be at the sub-ppb level. These results demonstrate that hydrogenation is effective for improving the sensing performance of graphene-based sensors.

See supplementary material for real-time response of the PGS measured repeatedly, Raman spectra of the OGS, FESEM images of graphene, and estimation of the LOD.

This work was financially supported by the Basic Science Research Program through the National Research Foundation of Korea (NRF) funded by the Ministry of Science, ICT and Future Planning (Grant Nos. 2016R1A2B3011980, 2014R1A2A1A11050290, and 2012R1A4A1029061).

[1]X. Li, W. Cai, J. An, S. Kim, J. Nah, D. Yang, R. Piner, A. Velamakanni, I. Jung, E. Tutuc, S. K. Banerjee, L. Colombo, and R. S. Ruoff, Science **324**, 1312 (2009).
[2]D. V. Kosynkin, A. L. Higginbotham, A. Sinitskii, J. R. Lomeda, A. Dimiev, B. K. Price, and J. M. Tour, Nature **458**, 872 (2009).
[3]D. Li and R. B. Kaner, Science **320**, 1170 (2008).
[4]T. Wang, D. Huang, Z. Yang, S. Xu, G. He, X. Li, N. Hu, G. Yin, D. He, and L. Zhang, Nano-Micro Lett. **8**, 95 (2016) and references therein.
[5]F. Schedin, A. K. Geim, S. V. Morozov, E. W. Hill, P. Blake, M. I. Katsnelson, and K. S. Novoselov, Nat. Mater. **6**, 652 (2007).
[6]A. Gutes, B. Hsia, A. Sussman, W. Mickelson, A. Zettl, C. Carraro, and R. Maboudian, Nanoscale **4**, 438 (2012).
[7]A. Salehi-Khojin, D. Estrada, K. Y. Lin, M.-H. Bae, F. Xiong, E. Pop, and R. I. Masel, Adv. Mater. **24**, 53 (2012).
[8]R. K. Paul, S. Badhulika, N. M. Saucedo, and A. Mulchandani, Anal. Chem. **84**, 8171 (2012).
[9]M. G. Chung, D. H. Kim, H. M. Lee, T. Kim, J. H. Choi, D. K. Seo, J. B. Yoo, S.-H. Hong, T. J. Kang, and Y. H. Kim, Sens. Actuators, B **166–167**, 172 (2012).
[10]J. Dai, J. Yuan, and P. Giannozzi, Appl. Phys. Lett. **95**, 232105 (2009).
[11]Y.-H. Zhang, Y.-B. Chen, K.-G. Zhou, C.-H. Liu, J. Zeng, H.-L. Zhang, and Y. Peng, Nanotechnology **20**, 185504 (2009).
[12]S. Bae, H. Kim, Y. Lee, X. Xu, J. S. Park, Y. Zheng, J. Balakrishnan, T. Lei, H. R. Kim, Y. I. Song, Y. J. Kim, K. S. Kim, B. Ozyilmaz, J. H. Ahn, B. H. Hong, and S. Iijima, Nat. Nanotechnol. **5**, 574 (2010).
[13]Y. Lee, S. Bae, H. Jang, S. Jang, S. E. Zhu, S. H. Sim, Y. I. Song, B. H. Hong, and J. H. Ahn, Nano Lett. **10**, 490 (2010).
[14]J. Son, S. Lee, S. J. Kim, B. C. Park, H. K. Lee, S. Kim, J. H. Kim, B. H. Hong, and J. Hong, Nat. Commun. **7**, 13261 (2016).
[15]A. Das, S. Pisana, B. Chakraborty, S. Piscanec, S. K. Saha, U. V. Waghmare, K. S. Novoselov, H. R. Krishnamurthy, A. K. Geim, A. C. Ferrari, and A. K. Sood, Nat. Nanotechnol. **3**, 210 (2008).
[16]D. J. Late, Y.-K. Huang, B. Liu, J. Acharya, S. N. Shirodkar, J. Luo, A. Yan, D. Charles, U. V. Waghmare, V. P. David, and C. N. R. Rao, ACS Nano **7**, 4879 (2013).
[17]Q. He, Z. Zeng, Z. Yin, H. Li, S. Wu, X. Huang, and H. Zhang, Small **8**, 2994 (2012).
[18]D. J. Late, R. V. Kanawade, P. K. Kannan, and C. S. Rout, Sens. Lett. **14**, 1249 (2016).
[19]A. Eckmann, A. Felten, A. Mishchenko, L. Britnell, R. Krupke, K. S. Novoselov, and C. Casiraghi, Nano Lett. **12**, 3925 (2012).
[20]I. Childres, L. A. Jauregui, J. Tian, and Y. P. Chen, New J. Phys. **13**, 025008 (2011).
[21]J. O. Sofo, A. S. Chaudhari, and G. D. Barber, Phys. Rev. B **75**, 153401 (2007).
[22]Y. Mulyana, M. Uenuma, Y. Ishikawa, and Y. Uraoka, J. Phys. Chem. C **118**, 27372 (2014).
[23]A. W. Adamson and A. P. Gast, *Physical Chemistry of Surfaces*, 6th ed. (Wiley, New York, 1997).